ENDOHEDRAL METALLOFULLERENES: ISOLATION AND CHARACTERIZATION

H. C. DORN,* S. STEVENSON,* P. BURBANK,* Z. SUN,* T. GLASS,* K. HARICH, * P. H. M. VAN LOOSDRECHT,+ R. D. JOHNSON,+ R. BEYERS,+ J. R. SALEM,+ M. S. DE VRIES,+ C. S. YANNONI,+ C. H. KIANG# AND D. S. BETHUNE,+
*Department of Chemistry, Virginia Tech, Blacksburg, VA 24061-0212
+IBM Almaden Research Center, San Jose, CA 95120-6099
#Materials and Molecular Simulation Ctr., Beckman Institute, Caltech, Pasadena, CA 91125

INTRODUCTION

Since the initial discovery of fullerenes nearly a decade ago [1], material scientists have focused attention on the possibility of encapsulating one or more metal atoms inside these spheroidal carbon frames. The experimental realization of macroscopic quantities of endohedral metallofullerenes ($A_m@C_{2n}$, n=30-55) in the early 1990's has heightened interest in developing this new class of tunable materials with possible electronic and/or optical applications [2,3]. They have been characterized by a number of spectroscopic techniques, for example, scanning tunneling microscope [4,5], EXAFS [6,7] and x-ray diffraction and electron microscopy [8]. However, low production yields and purification difficulties have hampered the development of this new class of materials. The soluble product distribution usually consists of high levels of the empty-caged fullerenes C_{60}, C_{70}, C_{84} and decreasing levels of the higher fullerenes, while the endohedral metallofullerene fraction usually constitutes less than 1% of the total soluble yield. Furthermore, the endohedral metallofullerene fraction consists of molecules with different numbers of metal atoms encapsulated (m=1-3), cage sizes (C_{2n}) and isomers of the same mass (e.g., $Er_2@C_{82}$). The purification process is further complicated by the chemical reactivity of several endohedral metallofullerenes [9] in aerobic environments. For several years, we have been involved in a collaborative effort to develop methodology for detection, isolation, and characterization of endohedral metallofullerenes. The focus of the present study is on fullerenes encapsulating metals from Group IIIb, ($Sc@C_{2n}$, $Y@C_{2n}$, and $La@C_{2n}$) and the lanthanide series metal ($Er@C_{2n}$).

PRODUCTION AND INITIAL SEPARATION PROCEDURES

The samples were produced by arc-burning cored carbon rods filled with mixtures of powdered carbon and pure metal or metal oxide. A Krätschmer-Huffman style fullerene generator [10] (I~100A, ~25V) was utilized to "burn" the rods and operated under a dynamic helium flow (~200 torr). Previous experiments have demonstrated that the yields and product distribution are relatively insensitive to the form in which the metal is introduced (metal, metal oxide, or carbide) [11]. However, the product distribution (and yield) is quite sensitive to the metal concentration. Monometal species dominate at low metal/carbon ratios whereas the di- and trimetal species dominate at high metal loadings (~3-4%). The fullerene containing soot was promptly extracted with cold CS_2 or with Soxhlet extraction using refluxing toluene.

Mat. Res. Soc. Symp. Proc. Vol. 359 © 1995 Materials Research Society

After solvent removal **in vacuo**, the soluble fullerene and metallofullerene extract was washed with diethyl ether.

An automated HPLC apparatus [12] has been extensively employed in the initial purification stages (Fig. 1). The C_1, C_2 and C_3, C_4 columns function as load columns and the separation columns, respectively. Both polystyrene (Perkin-Elmer PL gel, 1000 and 500 A°, 250 x 10 mm columns in series) and Buckyclutcher (Regis, Trident-Tri-DNP, 250 x 10 mm columns in series) have been used for the initial separation. The separation protocol used for the erbium metallofullerene ($Er@C_{2n}$) is typical and is described in more detail below. In a given automated sequence, injection of the soluble fullerene/metallofullerene extract (e.g., $Er_m@C_{2n}$, 5-7.5 ml, ~3 mg/ml) was separated with flow rates of 1 ml/min. (80/20, toluene/decalin mobile phase) and a 90 min recycle time. The low flow rates provide good separation with low solvent consumption. For a 24 hr period, an automated through-put in excess of 300 mg of the soluble metallofullerene extract can be achieved for the initial separation step.

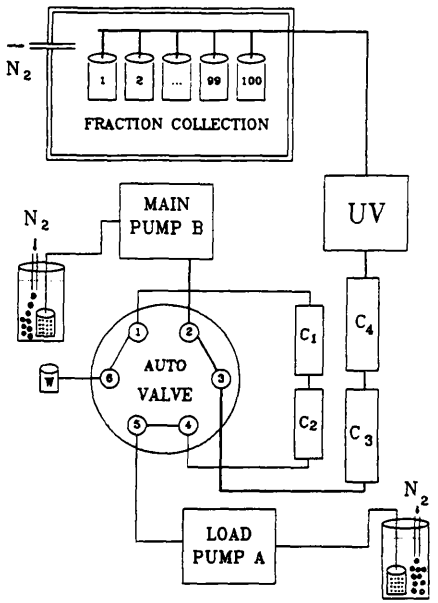

Figure 1. Automated HPLC Apparatus: C_1, C_2 are the load columns and C_3, C_4 are the separation (polystyrene or Buckyclutcher) columns [12].

ENDOHEDRAL SCANDIUM METALLOFULLERENES

It is now well established [5, 11-15] that $Sc_m@C_{2n}$ extracts contain the paramagnetic $Sc@C_{82}$ and $Sc_3@C_{82}$ species as well as numerous dimetal metallofullerenes (e.g., $Sc_2@C_{84}$). In addition, the usual empty-cage fullerenes (C_{60}, C_{70}, C_{76}, C_{84}, etc.) dominate the soluble product profile. Although UV detection (260-400 nm) is commonly used to monitor metallofullerene separations, on-line electron paramagnetic resonance (HPLC-EPR) has the

advantage of selective monitoring only the paramagnetic endohedral fullerenes ($Sc@C_{82}$ and $Sc_3@C_{82}$). The latter species provide convenient "markers" for the metallofullerene fraction. To illustrate the approach, the HPLC-UV trace and corresponding EPR profile for a $Sc@C_{2n}$ fraction is shown in Fig. 2 after five separate passes using polystyrene columns to remove most of the empty-cage fullerenes [16]. The characteristic 22 line hyperfine coupling (hfc) for the three equivalent Sc atoms inside the $Sc_3@C_{82}$ species clearly maximizes at 30.75 min. The $Sc_3@C_{82}$ provides a convenient marker for the metallofullerene fraction which can then be separated into a number of $Sc_m@C_{2n}$ species using a Buckyclutcher column (Fig. 3). Although there are several resolved peaks in this chromatogram, the HPLC-EPR profile clearly identifies peak 6 as the $Sc_3@C_{82}$ species. Additional clean-up passes of peak 6 readily permitted isolation of purified $Sc_3@C_{82}$. The negative-ion mass spectrum (m/e=1119) confirmed the assignment of $Sc_3@C_{82}$. A portion of this purified sample was used in the EPR orientational dynamics study of the Sc_3 trimer in $Sc_3@C_{82}$ described below.

In addition to the $Sc_3@C_{82}$ marker species, a number of other peaks in Fig. 3 were identified by negative-ion mass spectrometry. For example, peaks 0, 1, 3, and 5 have been identified as $Sc_2@C_{74}$, $Sc_2@C_{84}$ (I), $Sc_2@C_{84}$ (II), and $Sc_2@C_{76}$, respectively. At least three different isomers of $Sc_2@C_{84}$ are clearly evident from the mass spectral data (peaks 1, 3 and 9). Multiple isomers for several other dimetal species (e.g., $Er_2@C_{82}$) have been tentatively identified from mass spectral and HPLC retention data. The dominant $Sc_2@C_{84}$ isomer (Peak 3) was purified by additional clean-up passes. A portion of the purified $Sc_2@C_{84}$ sample was utilized in the electron microscopy study described below [8].

The $Sc_m@C_{2n}$ extract described above was prepared with a relatively high metal/carbon ratio (3-5 Sc atoms/100 carbon atoms) which accounts for the relatively minor abundance of $Sc@C_{82}$ in this sample. In a separate experiment, a $Sc_m@C_{2n}$ extract was prepared with a lower Sc/C ratio. The HPLC/EPR profile (Fig. 4) for this sample (Buckyclutcher column) demonstrates that $Sc@C_{82}$ has a slightly faster elution time (19 min) in comparison with $Sc_3@C_{82}$ (23 min). In this case, a slightly slower flow rate (2 ml/min) was employed in comparison with Fig. 3. Also, the characteristic 8 line pattern for $Sc@C_{82}$ is distorted because of saturation (excessive microwave power) in order to improve the signal-to-noise in the HPLC/EPR profile.

$Sc_2@C_{84}$ ELECTRON MICROSCOPY

Of primary importance regarding the structure of endohedral metallofullerenes is experimental verification that the metal atoms are indeed inside the carbon cage. In a recent electron microscopy study, a purified $Sc_2@C_{84}$ sample (Peak 3, Fig. 3) was allowed to slowly evaporate from CS_2 and placed on a carbon grid for transmission electron microscopy (TEM) [18]. The room temperature results show that $Sc_2@C_{84}$ molecules pack in a hexagonal-close-packed (HCP) structure with a ratio of lattice constants c/a=1.63, the value expected for ideal-sphere packing. The molecule spacing of 11.2 A° is close to the value found for empty-cage C_{84} [18] This suggests that the van der Waals radius of the molecules is not strongly altered by charge transfer to the carbon cage. High resolution TEM images taken along both the $[\bar{1}\bar{1}20]$ and [0001] directions confirm the HCP structure and show no bright central spots in the molecular images which would be expected for empty-cage fullerenes (C_{84}). A scanning tunneling microscope (STM) study of $Sc_2@C_{84}$ on a Si surface reported by Shinohara [5], also suggested the endohedral nature of this species. In their study, a nearest neighbor distance of 11.7A° was reported between the $Sc_2@C_{84}$ molecules.

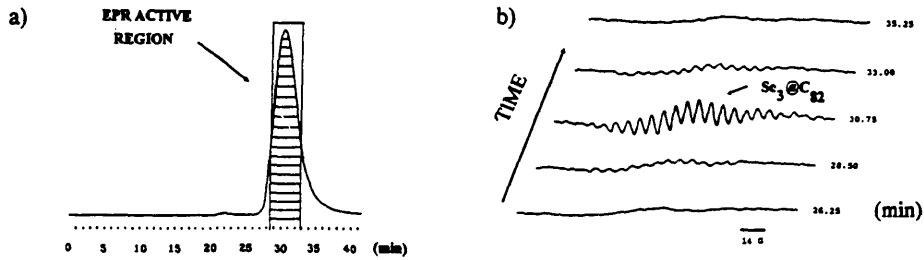

Figure 2. (a) HPLC-UV trace (340 nm) for the fifth polystyrene pass, 410-μL injection of the $Sc@C_{2n}$ EPR active fraction, 1 mL/min, and 80:20 degassed toluene/decalin. (b) On-line HPLC-EPR profile, 9.55 GHz, 4 scans/file, and 20 s/sweep [16].

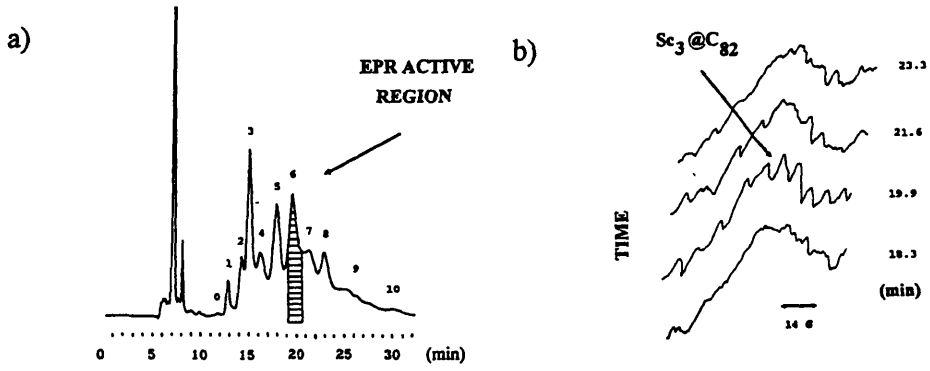

Figure 3. (a) HPLC-UV trace (340 nm), concentrated $Sc_3@C_{82}$ fraction after five polystyrene passes, Buckyclutcher column, 250-μL injection, 2.1 mL/min, and degassed 80:20 toluene/decalin; EPR-active region is peak 6. (b) On-line HPLC-EPR stacked plot, 9.55 GHz, 3 scans/file, and 20 s/sweep [16].

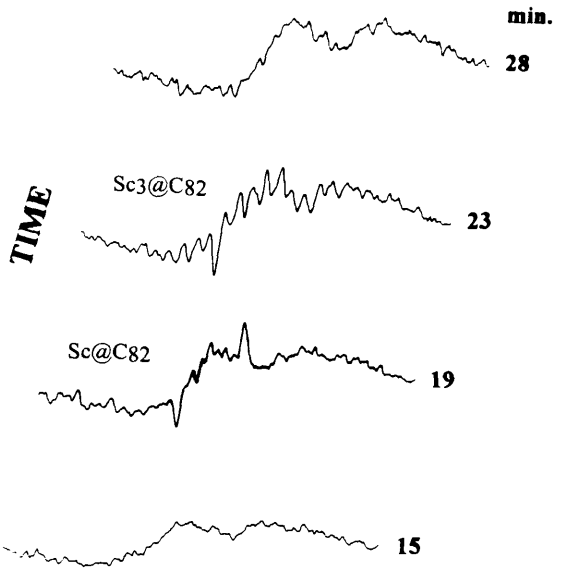

Figure 4. On-line HPLC-EPR profile for $Sc_m@C_{2n}$ extract 2.0 ml/min, degassed 80:20 toluene/decalin; EPR 9.55 GHz, 3 scans/file and 20 s/sweep.

ORIENTATIONAL DYNAMICS OF THE Sc_3 TRIMER IN $Sc_3@C_{82}$: AN EPR STUDY

The highly anharmonic potential for the metal atoms in metallofullerenes leads to the expectation that these species will exhibit novel dynamical properties. Calculations have predicted new types of vibrations for endohedral fullerenes, with the encapsulted atoms rattling and rolling inside the cage. We have carried out a systematic study of the electron paramagnetic resonance (EPR) spectrum of $Sc_3@C_{82}$ for temperatures varying from 77 K to 333 K that gives new information about the dynamical behavior of this species [17]. The study was carried out on a purified sample of $Sc_3@C_{82}$ [16]. The EPR spectra show 22 hyperfine coupling split transitions with unusually large linewidths [18,19]. Figure 5a and 5b show two spectra taken at 193 K in decalin. The spectrum in Fig. 5a was obtained with the solvent supercooled, but still liquid. The spectrum in Fig. 5b was taken with the solvent frozen. In both cases, the data show that the three Sc ions are equivalent, and can be modeled using a simulation with equal isotropic hyperfine coupling to the three scandium nuclei. As the temperature falls, there is a strongly m-dependent broadening of the lines, with the linewidths increasing as -|m|. The effect of this broadening is evident in Fig. 5b. As shown in Figure 6, the linewidth has the qualitative temperature dependence expected for a paramagnetic species tumbling in solution due to Brownian motion: the linewidth increases at low temperatures due to insufficient averaging of the magnetic anisotropy by reorientational motions, whereas at high temperatures the linewidth increases due to the interactions between

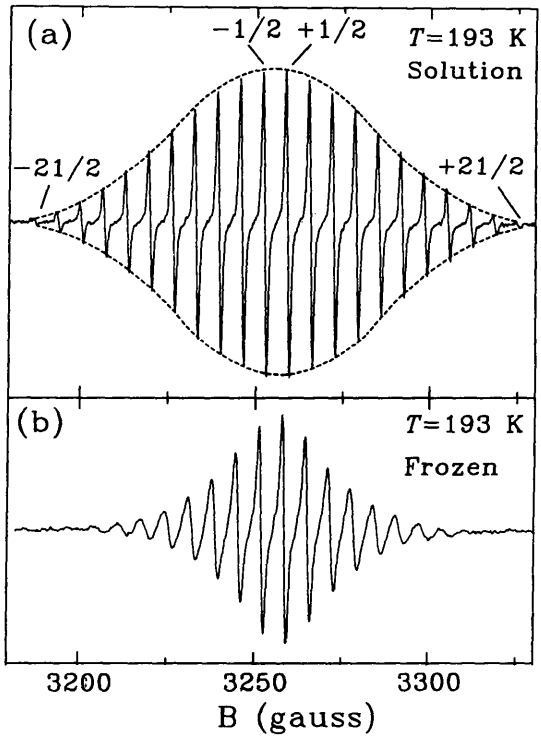

Figure 5. EPR spectrum of $Sc_3@C_{82}$ in (a) fluid and (b) frozen decalin at T=193 K. Some of the nuclear magnetic quantum numbers of the states involved in the transitions are indicated in (a). The dashed line is the envelope of a simulation of the fluid spectrum. (c) Simulation of the frozen spectrum.

the unpaired spin and the magnetic moment associated with rapid molecular rotation. However, the temperature dependence of the linewidth strongly deviates from that expected to result from the Brownian tumbling motion of the C_{82} cage (shown by the dashed line in Fig. 6): at high temperatures the observed linewidths are too large compared to the value expected for spin-rotation interaction due to cage reorientation, whereas at low temperatures (where the cage motion becomes very slow), the linewidths are much too small. Even in frozen decalin resolved hyperfine structure persists, indicating there still is rapid reorientational averaging. These results contrast sharply with those obtained for $Sc@C_{82}$ by Kato et al., which seem to follow expectations for broadening due to cage rotation [20]. We were thus led to consider broadening due to motion of the Sc trimer within the fullerene cage. We postulated that the metal trimer can reorient by overcoming a barrier to rotation **E**, resulting in a correlation time for trimer reorientation proportional to $\mathbf{exp(E/kT)}$. The reorientation of the cage in the viscous solvent was assumed to be described by a second correlation time proportional to the viscosity and $\mathbf{T^{-1}}$ in the usual way. By thus considering both motion of the cage in solution

and of the Sc trimer within the cage, the data could be fit across the full measured temperature range, for both liquid and frozen solvent, as shown by the solid lines in Fig. 6. A small barrier to trimer reorientation (28 meV) is derived from the data. An additional consequence of the Sc_3 reorientational motion is that the hyperfine coupling, **a(hfc)**, will be modulated as the trimer moves. The observed hyperfine coupling will be an averaged value that will depend on the magnetic quantum number m and on the temperature. Indeed, **a(hfc)** varies with m and, as shown in Figure 7, has a strong temperature dependence - varying by 10% over the range from 100 to 325 K. This evidence of large amplitude motion strongly supports the notion of facile Sc trimer reorientation. The conclusion that the Sc metal trimer can move rapidly with respect to the cage lends support to the idea that the unusual structure of these species will lead to unusual linear and nonlinear polarizabilities and vibrational properties [21,22].

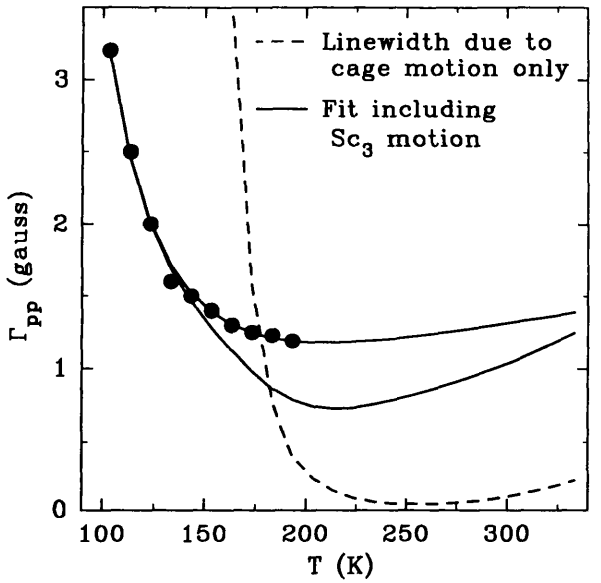

Figure 6. Temperature dependence of the linewidth of the m_i=+1/2 (see Fig. 1) EPR transitions for $Sc_3@C_{82}$ in frozen (filled circles) and fluid (open circles) decalin. The solid lines are fits of a dynamical model.

$Er_2@C_{82}$ ISOMERS

In contrast with $Sc_m@C_{2n}$, $Y_m@C_{2n}$, and $La_m@C_{2n}$, erbium metallofullerene extracts are dominated by only $Er@C_{82}$, $Er_2@C_{82}$ and smaller quantities of $Er_2@C_{84}$, as shown in the LD-TOF mass spectrum (Fig. 8). Isolation of $Er_2@C_{82}$ was accomplished in a four-stage automated chromatographic procedure. The initial separation stage using two Buckyclutcher columns (250 x 10 mm) with a toluene/decalin (80/20) solvent system has been previously described ***vide supra***. After a second automated pass using the same chromatographic procedure, the enriched $Er_2@C_{82}$ fraction (Fig. 9) shows three major peaks I, II, and III

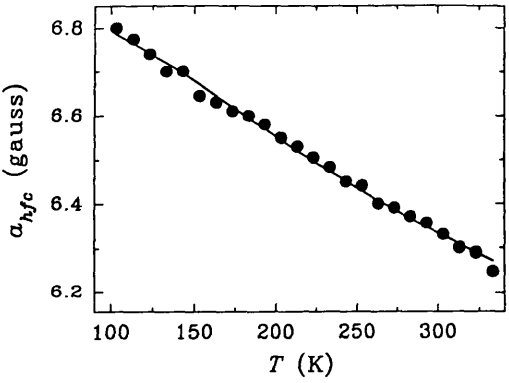

Figure 7. Temperature dependence of the nuclear hyperfine coupling observed for $Sc_3@C_{82}$ in liquid and frozen decalin. The solid line is a fit to the data of the dynamical model discussed in the text.

which were confirmed by LD-TOF mass spectrometry to be $Er_2@C_{82}$ and $Er_2@C_{84}$ (mixture), $Er_2@C_{82}$ and $Er_2@C_{82}$, respectively. However, low levels of empty-cage fullerenes, C_{100}-C_{106} were also found to be present in these fractions. To remove these empty-cage impurities, a tetraphenyl-porphyrin (TPP) derivatized silica-gel column (4.6 x 100 mm, Anspec) was used with the automated HPLC apparatus and with CS_2 as the mobile phase (Fig. 10). Under these conditions, the elution time of the empty-cage fullerene impurities (C_{100}-C_{106}) are considerably longer than the $Er_2@C_{82}$ isomers. After a final pass on the Buckyclutcher column, highly purified samples of $Er_2@C_{82}$ isomers II and III have been obtained. The LD-TOF mass spectrum for the $Er_2@C_{82}$ isomer III is illustrated in Fig. 11. From ~1.4 g of soluble $Er_m@C_{2n}$ extract, we have isolated ~9 mg of purified isomer III. Since isomer III is only ~1/3 of the total $Er_2@C_{82}$ product profile, the overall yield of $Er_2@C_{82}$ is significantly greater than 1% of the total soluble $Er_m@C_{2n}$ extract. The relative high abundance of $Er_2@C_{82}$ (as well as $Er@C_{82}$) in this extract is in sharp contrast with the lower yields and greater diversity of metallofullerene products typically found for $La_m@C_{2n}$, $Sc_m@C_{2n}$, and $Y_m@C_{2n}$ extracts.

The UV/Vis/NIR spectra for the isomers of $Er_2@C_{82}$ (I, II, and III) in CS_2 are shown in Fig. 12. Several sharp peaks are clearly evident for isomer III at 650, 900, and 1070 nm. The peak at ~900 nm appears in the spectra for all three isomers although it is less prominant in isomer I (which is contaminated with $Er_2@C_{84}$). The absorption onset for isomer III at 1150 nm suggests a HOMO-LUMO energy gap of ~1.1 EV, which is comparable to that for $Sc_3@C_{82}$ [15]. This is a much lower wavelength than observed for the open-shell monometal species, $La@C_{82}$, $Pr@C_{82}$, and $Gd@C_{82}$ [5, 23, 24]. For example, the threshold (~2000 nm) for $La@C_{82}$ is well into the near IR region [23]. In contrast, $Sc_2@C_{84}$, $La_2@C_{80}$, and $Sc_2@C_{82}$ exhibit broad spectral features with lower wavelength absorption onsets [7 ,13]. For example, $Sc_2@C_{84}$ has an absorption onset of ~800 nm [13]. The longer wavelength onset for $La@C_{82}$ has been interpreted in terms of cluster formation of the monometal species [15]. This argument suggests that dimer or cluster formation is not occuring for the di- and

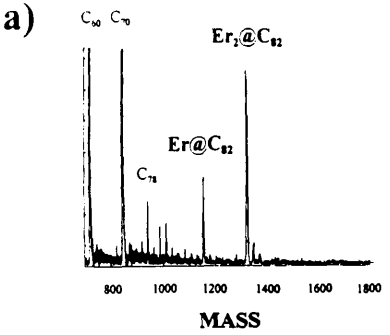

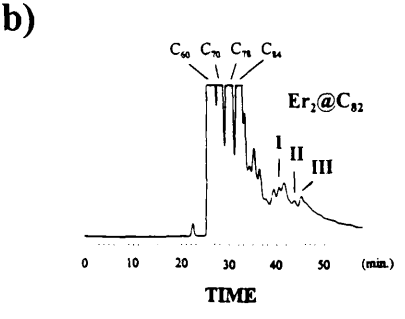

Figure 8. (a) LD-TOF mass spectrum of $Er_m@C_{2n}$ raw extract. (b) $Er_m@C_{2n}$ stock solution chromatogram, 200 μL injection (Buckyclutcher column), 1.2 mL/min, toluene/decalin (80/20), and UV detection at 354 nm.

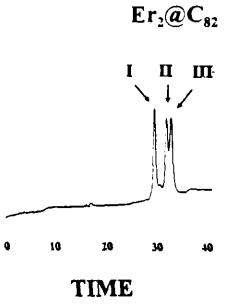

Figure 9. Chromatogram of $Er_2@C_{82}$ isomers I, II, and III. Buckyclutcher columns, 1.55 mL/min, toluen/decalin (80/20), and 340 nm UV detection.

trimetal endohedral metallofullerene species. Further efforts to characterize the purified $Er_2@C_{82}$ isomers (e.g. by ^{13}C NMR) are presently in progress.

TRENDS IN $A_m@C_{2n}$ SEPARATIONS

The quantities of endohedral metallofullerenes currently available still limit reactivity, complexation, and intermolecular collisional studies of these species with other substrate molecules. However, chromatographic stationary phases (e.g., Buckyclutcher and TPP) are known to provide a source of weak π-π complexation with substrate aromatic systems. For example, the Buckyclutcher stationary phase consists of a tripodal 3,5-dinitrobenzoate ester phase which can function as a weak π-acidic group. We have carefully evaluated the chromatographic retention behavior of a wide range of fullerenes (C_{60}-C_{100}) and several endohedral metallofullerenes ($Sc_m@C_{2n}$, $Y_m@C_{2n}$, $La_m@C_{2n}$, and $Er_m@C_{2n}$). The

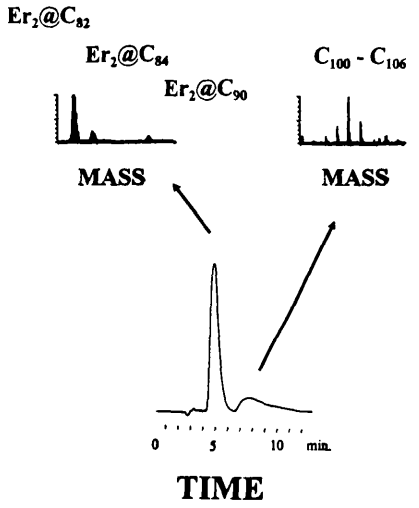

Figure 10. HPLC-UV trace for $Er_2@C_{82}$ fractions obtained from initial Buckyclutcher separation (Figure 9). Chromatographic conditions: TPP column, 1.0 mL/min CS_2, and 340 nm UV detection.

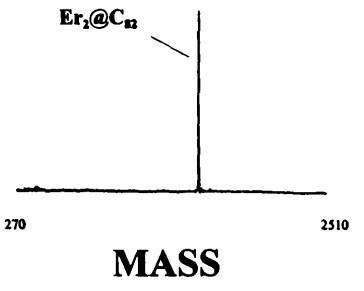

Figure 11. LD-TOF mass spectrum for $Er_2@C_{82}$ Isomer III.

chromatographic retention parameter, the capacity factor k', was determined for the Buckyclutcher and polystyrene stationary phases using the solvent system toluene/decalin (80/20). A capacity factor (log k') versus fullerene carbon number plot is illustrated in Fig. 13. As expected, the empty-cage fullerenes constitute a linear homologous series (slope=0.018) with log k' versus the number of carbons in the cage. For clarity, only the $A_m@C_{82}$ endohedral metallofullerenes are included in this figure. In all cases, the retention times of a given species were unambigously determined either by on-line HPLC-EPR and/or sample collection with off-line mass spectrometry. From a practical separation viewpoint, this plot is useful in determining which empty-cage fullerenes will co-elute with a given endohedral metallofullerene. For example, $Sc_3@C_{82}$ co-elutes with empty-cage fullerenes around of C_{112}. In contrast, $Y@C_{82}$ will be contaminated with empty-cage fullerenes centered at ~C_{104}. From a viewpoint of understanding the weak π-π complexation interaction of the stationary phase and the endohedral metallofullerene, clearly $Sc_3@C_{82}$ is more strongly retained than any of the monometal species ($Sc@C_{82}$, $Y@C_{82}$ and $La@C_{82}$). As a group, the dimetal species ($Sc_2@C_{82}$, $Y_2@C_{82}$, $La_2@C_{82}$ and $Er_2@C_{82}$) have similar retention times, but are generally the most weakly retained endohedral metallofullerenes. There are obvious minor differences in the retention times of the various isomers (e.g., $Er_2@C_{82}$, isomers I, II and III), but the retention times of the dimetal species are not significantly influenced by which metal atoms are in the cage or isomer differences. A similar plot for the weaker complexing polystyrene stationary phase exhibits the same overall trends, with a much lower slope (slope=0.0088) for the linear plot of empty-cage fullerenes. In addition, significantly reduced k' values for the endohedral metallofullerenes were observed. The lack of significant chromatographic

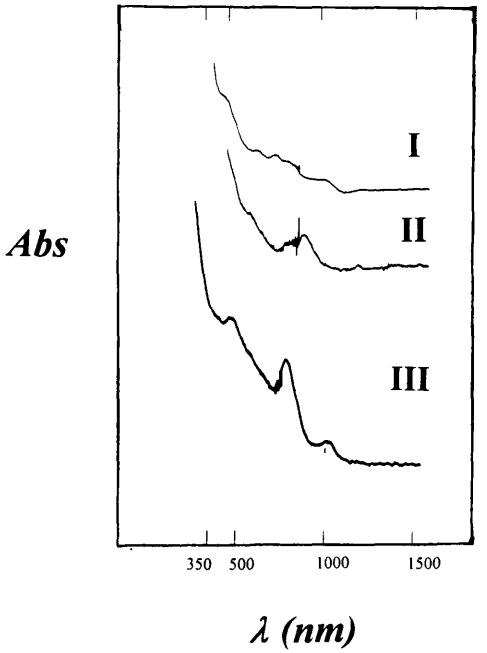

Figure 12. UV/Vis/NIR spectra for $Er_2@C_{82}$ Isomers I, II, and III.

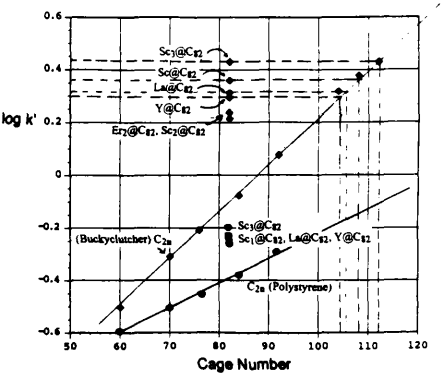

Figure 13. Chromatographic capacity factor (k') versus carbon cage number, ♦, (Buckyclutcher column, •, polystyrene column, 80/20 toluene/decalin mobile phase.

resolution of the individual endohedral species (e.g., small differences in k' for $Sc_3@C_{82}$ versus $Sc@C_{82}$) on this chromatographic phase clearly illustrates why these paramagnetic species served as ideal "markers" for the entire metallofullerene fraction under the conditions used in the earlier phases of this study, as described above.

CONCLUSION

This study illustrates the continued development of improved separation and detection (on-line EPR) methodology applicable to endohedral metallofullerenes. The characterization techniques (TEM, EPR, UV/Vis) provide a better understanding of the structure and dynamics (e.g., Sc_3 trimer) of these fascinating molecules. The preparation and isolation of purified $Er_2@C_{82}$ isomers in macroscopic quantities should ultimately provide new insight regarding the optical and electronic properties of these new materials.

ACKNOWLEDGEMENTS

We gratefully acknowledge stimulating discussions with Paul Kasai and Ray Kendrick. PvL gratefully acknowledges financial support by the Dutch Organization for Scientific Research (NWO) and the IBM Corporation. HCD gratefully acknowledges support from IBM Corporation and the Virginia Center for Innovative Technology. CHK gratefully acknowledges partial support by the NSF (ASC-9217368) and by the Materials and Molecular Simulation Center.

REFERENCES

1. H. W. Kroto, J. R. Heath, S. C. O'Brien, R. F. Curl and R. E. Smalley, *Nature* **218**, 162 (1985).
2. D. S. Bethune, R. D. Johnson, J. R. Salem, M. S. de Vries and C. S. Yannoni, *Nature* **366**, 123 (1993).
3. H. Schwarz, T. Weiske, D. K. Böhme and J. Hrusak, in *Buckminsterfullerenes*, eds. W. E. Billups and M. A. Ciufolini, VCH publishers, New York (1993), p. 257.
4. H.-D. Wang, Q. K. Xue, T. Hashizume, H. Shinohara, Y. Nishima and T. Sakurai, Phys. Rev. B **48**, 15492 (1993).
5. H. Shinohara, M. Kishida, T. Nakane, T. Kato, S. Bandow, Y. Saito, X-D. Wang, T. Hashizume and T. Sakurai, in *Fullerenes: Recent Advances in the Chemistry and Physics of Fullerenes and Related Materials*, (eds. Kadish, K. M. and Ruoff, R. S.), 1361-1381, (Electrochem. Soc., NJ, 1994).
6. C-H. Park, B. O. Wells, J. DiCarlo, Z-X. Shen, J. R. Salem, D. S. Bethune, C. S. Yannoni, R. D. Johnson, M. S. de Vries, C. Booth, F. Bridges and P. Pianetta, *Chem. Phys. Lett.* **213**, 196 (1993).
7. K. Kikuchi, Y. Nakao, Y. Achiba, M. Nomura, in *Fullerenes: Recent Advances in the Chemistry and Physics of Fullerenes and Related Materials*, (eds. Kadish, K. M. and Ruoff, R. S.), 1300-1308, (Electrochem. Soc., NJ, 1994).
8. R. Beyers, C-H. Kiang, R. D. Johnson, J. R. Salem, M. S. de Vries, C. S. Yannoni, D. S. Bethune, H. C. Dorn, P. Burbank, K. Harich and S. Stevenson, *Nature* **370**, 196 (1994).

9. S. Bandow, H. Kitagawa, T. Mitani, H. Inokuchi, Y. Saito, H. Yamaguchi, N. Hayashi, H. Sato and H. Shinohara, *J. Phys. Chem.* **96**, 9609 (1992).
10. W. Krätschmer, L. D. Lamb, K. Fostiropoulos and D. R. Huffman, *Nature* **347**, 354 (1990).
11. P. H. M. van Loosdrecht, R. D. Johnson, R. Beyers, J. R. Salem, M. S. de Vries, D. S. Bethune, P. Burbank, J. Haynes, T. Glass, S. Stevenson, H. C. Dorn, M. Boonman, P. J. M. van Bentum, G. Meijer, in *Fullerenes: Recent Advances in the Chemistry and Physics of Fullerenes and Related Materials*, (eds. Kadish, K. M. and Ruoff, R. S.), 1309-1319, (Electrochem. Soc., NJ, 1994).
12. S. Stevenson, H. C. Dorn, P. Burbank, K. Harich, J. Haynes, C-H. Kiang, J. R. Salem, M. S. de Vries, P. H. M. van Loosdrecht, R. D. Johnson, C. S. Yannoni, D. S. Bethune, *Anal. Chem.* **66**, 2675-2679 (1994).
13. H. Shinohara, H. Yamaguchi, H., N. Hayashi, H. Sato, M. Ohkohchi, Y. Ando and Y. Saito, *J. Phys. Chem.* **97**, 4259-4261 (1993).
14. H. Shinohara, H. Sato, M. Ohkohchi, Y. Ando, T. Kodama, T. Shida, T. Kato and Y. Saito, *Nature* **357**, 52-54 (1992).
15. H. Shinohara, M. Inakuma, N. Hayashi, H. Sato, Y. Saito, T. Kato and S. Bandow, *J. Phys. Chem.* **98**, 8597-8599 (1994).
16. S. Stevenson, H. C. Dorn, P. Burbank, K. Harich, Z. Sun, C-H Kiang, J. R. Salem, M. S. de Vries, P. H. M. van Loosdrecht, R. D. Johnson and C. S. Yannoni, *Anal. Chem.* **66**, 2680-2685 (1994).
17. P. Y. M. van Loosdrecht, R. D. Johnson, M. S. de Vries, D. S. Bethune, H. C. Dorn, P. Burbank and S. Stevenson, *Phys. Rev. Lett.* **23**, 3415-3418.
18. H. Shinohara, H. Sato, M. Ohkohchi, Y. Ando, T. Kodama, T. Shida, T. Kato, and Y. Saito, *Nature* **357**, 52-54 (1992).
19. C. S. Yannoni, M. Hoinkis, M. S. de Vries, D. S. Bethune, J. R. Salem, M. S. Crowder and R. D. Johnson, *Science* **256**, 1191-1192 (1992).
20. T. Kato, S. Suzuki, K. Kikuchik and Y. Achiba, *J. Phys. Chem.* **97**, 13425-13428 (1993).
21. P. P. Schmidt, B. I. Dunlap and C. T. White, *J. Phys. Chem.* **95**, 10537-10541 (1991).
22. C. G. Joslin, J. Yang, C. G. Gray, S. Goldman and J. D. Poll, *Chem. Phys. Lett.* **208**, 86-92 (1993).
23. K. Kikuchi, S. Suzuki, Y. Nakao, N. Nakahara, T. Wakabayashi, H. Shiromaru, K. Saito, I. Ikemoto and Y. Achiba, *Chem. Phys. Lett.* **216**, 67-71 (1993).
24. K. Yamamoto, H. Funasaka, T. Takahashi and T. Akasaka, *J. Phys. Chem.* **98**, 2008-2011 (1994).